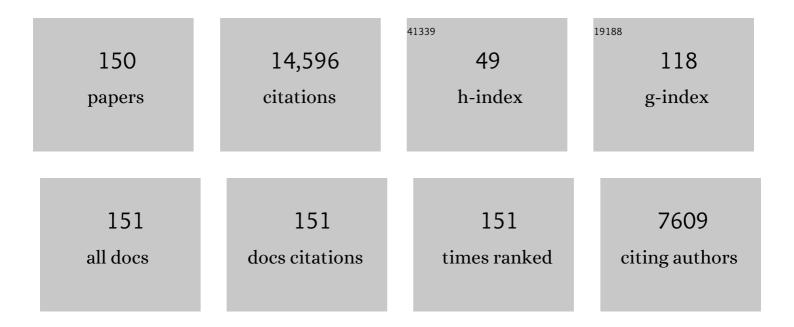
Gary D Egbert

List of Publications by Year in descending order

Source: https://exaly.com/author-pdf/7792099/publications.pdf Version: 2024-02-01



CADY D FOREDT

#	Article	IF	CITATIONS
1	An efficient multigrid solver based on a four-color cell-block Gauss-Seidel smoother for 3D magnetotelluric forward modeling. Geophysics, 2022, 87, E121-E133.	2.6	17
2	Baroclinic Tidal Energetics Inferred from Satellite Altimetry. Journal of Physical Oceanography, 2022, 52, 1015-1032.	1.7	6
3	Fluid transport and storage in the Cascadia forearc influenced by overriding plate lithology. Nature Geoscience, 2022, 15, 677-682.	12.9	13
4	Accuracy assessment of global internal-tide models using satellite altimetry. Ocean Science, 2021, 17, 147-180.	3.4	28
5	Magnetotelluric Data Processing. Encyclopedia of Earth Sciences Series, 2021, , 1036-1042.	0.1	0
6	3-D time-domain electromagnetic modeling based on multi-resolution grid with application to geomagnetically induced currents. Physics of the Earth and Planetary Interiors, 2021, 312, 106651.	1.9	5
7	Electrical conductivity of the lithosphere-asthenosphere system. Physics of the Earth and Planetary Interiors, 2021, 313, 106661.	1.9	10
8	A Comparison Study of Explicit and Implicit 3-D Transient Electromagnetic Forward Modeling Schemes on Multi-Resolution Grid. Geosciences (Switzerland), 2021, 11, 257.	2.2	1
9	The problematic <i>î⁻</i> 1 ocean tide. Geophysical Journal International, 2021, 227, 1181-1192.	2.4	3
10	Modelling diurnal variation magnetic fields due to ionospheric currents. Geophysical Journal International, 2021, 225, 1086-1109.	2.4	12
11	Electrical resistivity imaging of continental United States from three-dimensional inversion of EarthScope USArray magnetotelluric data. Earth and Planetary Science Letters, 2021, 576, 117244.	4.4	17
12	An Approach to Empirical Mapping of Incoherent Internal Tides With Altimetry Data. Geophysical Research Letters, 2021, 48, e2021GL095863.	4.0	6
13	An Efficient Preconditioner for 3-D Finite Difference Modeling of the Electromagnetic Diffusion Process in the Frequency Domain. IEEE Transactions on Geoscience and Remote Sensing, 2020, 58, 500-509.	6.3	21
14	3-D DC Resistivity Forward Modeling Using the Multi-resolution Grid. Pure and Applied Geophysics, 2020, 177, 2803-2819.	1.9	8
15	Modular finite volume approach for 3D magnetotelluric modeling of the Earth medium with general anisotropy. Physics of the Earth and Planetary Interiors, 2020, 309, 106585.	1.9	14
16	Array analysis of magnetic and electric field observatories in China: estimation of magnetotelluric impedances at very long periods. Geophysical Journal International, 2020, 222, 305-326.	2.4	2
17	3â€D Magnetotelluric Imaging of the Easternmost Kunlun Fault: Insights Into Strain Partitioning and the Seismotectonics of the Jiuzhaigou Ms7.0 Earthquake. Journal of Geophysical Research: Solid Earth, 2020, 125, e2020JB019731.	3.4	27
18	Magnetotelluric Data Processing. Encyclopedia of Earth Sciences Series, 2020, , 1-7.	0.1	0

#	Article	IF	CITATIONS
19	Constraints on the resistivity of the oceanic lithosphere and asthenosphere from seafloor ocean tidal electromagnetic measurements. Geophysical Journal International, 2019, 219, 464-478.	2.4	9
20	Insights Into Intraplate Stresses and Geomorphology in the Southeastern United States. Geophysical Research Letters, 2019, 46, 8711-8720.	4.0	8
21	The Missouri High-Conductivity Belt, revealed by magnetotelluric imaging: Evidence of a trans-lithospheric shear zone beneath the Ozark Plateau, Midcontinent USA?. Tectonophysics, 2019, 753, 111-123.	2.2	17
22	Synthesizing Seemingly Contradictory Seismic and Magnetotelluric Observations in the Southeastern United States to Image Physical Properties of the Lithosphere. Geochemistry, Geophysics, Geosystems, 2019, 20, 2606-2625.	2.5	10
23	A block rational Krylov method for 3-D time-domain marine controlled-source electromagnetic modelling. Geophysical Journal International, 2019, 218, 100-114.	2.4	19
24	Corrections to "An Efficient Preconditioner for 3D Finite Difference Modeling of the Electromagnetic Diffusion Process in the Frequency Domain―[DOI: 10.1109/TGRS.2019.2937742]. IEEE Transactions on Geoscience and Remote Sensing, 2019, 57, 9512-9512.	6.3	0
25	3-D DC resistivity modeling and inversion using multi-resolution framework. ASEG Extended Abstracts, 2019, 2019, 1-3.	0.1	1
26	Divergence-free solutions to electromagnetic forward and adjoint problems: a regularization approach. Geophysical Journal International, 2019, 216, 906-918.	2.4	30
27	A multi-resolution approach to electromagnetic modelling. Geophysical Journal International, 2018, 214, 656-671.	2.4	26
28	Shared advances in exploration and fundamental geophysics — Introduction. Geophysics, 2018, 83, WCi-WCii.	2.6	0
29	Modular implementation of magnetotelluric 2D forward modeling with general anisotropy. Computers and Geosciences, 2018, 118, 27-38.	4.2	17
30	Source biases in midlatitude magnetotelluric transfer functions due to Pc3-4 geomagnetic pulsations. Earth, Planets and Space, 2018, 70, .	2.5	14
31	A novel CFSâ€₱ML boundary condition for transient electromagnetic simulation using a fictitious wave domain method. Radio Science, 2017, 52, 118-131.	1.6	13
32	Electrical conductivity structure of southeastern North America: Implications for lithospheric architecture and Appalachian topographic rejuvenation. Earth and Planetary Science Letters, 2017, 462, 66-75.	4.4	54
33	3-D inversion of complex magnetotelluric data from an Archean-Proterozoic terrain in northeastern São Francisco Craton, Brazil. Geophysical Journal International, 2017, 210, 1545-1559.	2.4	11
34	An application of principal component analysis to the interpretation of ionospheric current systems. Journal of Geophysical Research: Space Physics, 2017, 122, 5687-5708.	2.4	15
35	Methodology for timeâ€domain estimation of storm time geoelectric fields using the 3â€D magnetotelluric response tensors. Space Weather, 2017, 15, 874-894.	3.7	59
36	Tidal Prediction. Journal of Marine Research, 2017, 75, 189-237.	0.3	34

#	Article	IF	CITATIONS
37	Coastal ocean variability in the US Pacific Northwest region: seasonal patterns, winter circulation, and the influence of the 2009–2010 El Niño. Ocean Dynamics, 2015, 65, 1643-1663.	2.2	17
38	lonospheric current source modeling and global geomagnetic induction using ground geomagnetic observatory data. Journal of Geophysical Research: Solid Earth, 2015, 120, 6771-6796.	3.4	35
39	Three-dimensional electrical resistivity of the north-central USA from EarthScope long period magnetotelluric data. Earth and Planetary Science Letters, 2015, 422, 87-93.	4.4	88
40	3-D joint inversion of the magnetotelluric phase tensor and vertical magnetic transfer functions. Geophysical Journal International, 2015, 203, 1128-1148.	2.4	39
41	An improved parameterization of tidal mixing for ocean models. Geoscientific Model Development, 2014, 7, 211-224.	3.6	18
42	Accuracy assessment of global barotropic ocean tide models. Reviews of Geophysics, 2014, 52, 243-282.	23.0	338
43	Time-Variable Refraction of the Internal Tide at the Hawaiian Ridge. Journal of Physical Oceanography, 2014, 44, 538-557.	1.7	73
44	ModEM: A modular system for inversion of electromagnetic geophysical data. Computers and Geosciences, 2014, 66, 40-53.	4.2	521
45	Intensified Diurnal Tides along the Oregon Coast. Journal of Physical Oceanography, 2014, 44, 1689-1703.	1.7	12
46	Deep electrical resistivity structure of the northwestern U.S. derived from 3-D inversion of USArray magnetotelluric data. Earth and Planetary Science Letters, 2014, 402, 290-304.	4.4	208
47	Implementing novel schemes for inversion of 3D EM data in ModEM, the OSU modular EM inversion system. , 2014, , .		0
48	Reply to comments by S. R. Dickman on †Fortnightly Earth rotation, ocean tides and mantle anelasticity'. Geophysical Journal International, 2013, 192, 1055-1058.	2.4	0
49	Cabled marine magnetotellurics: Denser data at lower cost and higher information content. , 2013, , .		0
50	Crust and upper mantle electrical conductivity beneath the Yellowstone Hotspot Track. Geology, 2012, 40, 447-450.	4.4	76
51	Spherical decomposition of electromagnetic fields generated by quasi-static currents. GEM - International Journal on Geomathematics, 2012, 3, 279-295.	1.6	8
52	Variational assimilation of HF radar surface currents in a coastal ocean model off Oregon. Ocean Modelling, 2012, 49-50, 86-104.	2.4	33
53	Computational recipes for electromagnetic inverse problems. Geophysical Journal International, 2012, 189, 251-267.	2.4	562
54	Fortnightly Earth rotation, ocean tides and mantle anelasticity. Geophysical Journal International, 2012, 189, 400-413.	2.4	30

#	Article	IF	CITATIONS
55	A thin-sheet model for global electromagnetic induction. Geophysical Journal International, 2012, 189, 343-356.	2.4	19
56	Hybrid conjugate gradient-Occam algorithms for inversion of multifrequency and multitransmitter EM data. Geophysical Journal International, 2012, 190, 255-266.	2.4	13
57	Robust principal component analysis of electromagnetic arrays with missing data. Geophysical Journal International, 2012, 190, 1423-1438.	2.4	31
58	Variational assimilation of satellite observations in a coastal ocean model off Oregon. Journal of Geophysical Research, 2011, 116, .	3.3	41
59	Application of 3D inversion to magnetotelluric profile data from the Deccan Volcanic Province of Western India. Physics of the Earth and Planetary Interiors, 2011, 187, 33-46.	1.9	57
60	Spatial and Temporal Variability of the M2 Internal Tide Generation and Propagation on the Oregon Shelf. Journal of Physical Oceanography, 2011, 41, 2037-2062.	1.7	42
61	Tide Predictions in Shelf and Coastal Waters: Status and Prospects. , 2011, , 191-216.		50
62	Magnetotelluric Data Processing. Encyclopedia of Earth Sciences Series, 2011, , 816-822.	0.1	2
63	Combined Effects of Wind-Driven Upwelling and Internal Tide on the Continental Shelf. Journal of Physical Oceanography, 2010, 40, 737-756.	1.7	35
64	Longâ€ŧerm monitoring of ULF electromagnetic fields at Parkfield, California. Journal of Geophysical Research, 2010, 115, .	3.3	26
65	Assimilation of altimetry data for nonlinear shallow-water tides: Quarter-diurnal tides of the Northwest European Shelf. Continental Shelf Research, 2010, 30, 668-679.	1.8	111
66	Representer-based analyses in the coastal upwelling system. Dynamics of Atmospheres and Oceans, 2009, 48, 198-218.	1.8	25
67	Baroclinic tidal generation in the Kauai Channel inferred from high-frequency radio Doppler current meters. Dynamics of Atmospheres and Oceans, 2009, 48, 93-120.	1.8	23
68	WSINV3DMT: Vertical magnetic field transfer function inversion and parallel implementation. Physics of the Earth and Planetary Interiors, 2009, 173, 317-329.	1.9	155
69	Assimilation of GRACE tide solutions into a numerical hydrodynamic inverse model. Geophysical Research Letters, 2009, 36, .	4.0	18
70	A nested grid model of the Oregon Coastal Transition Zone: Simulations and comparisons with observations during the 2001 upwelling season. Journal of Geophysical Research, 2009, 114, .	3.3	26
71	Global electromagnetic induction constraints on transition-zone water content variations. Nature, 2009, 460, 1003-1006.	27.8	219
72	Non-linear conjugate gradient inversion for global EM induction: resolution studies. Geophysical Journal International, 2008, 173, 365-381.	2.4	84

#	Article	IF	CITATIONS
73	Regional conductivity structure of Cascadia: Preliminary results from 3D inversion of USArray transportable array magnetotelluric data. Geophysical Research Letters, 2008, 35, .	4.0	73
74	Normal-Mode Instabilities of a Time-Dependent Coastal Upwelling Jet. Journal of Physical Oceanography, 2008, 38, 2056-2071.	1.7	7
75	The Inverse Ocean Modeling System. Part II: Applications. Journal of Atmospheric and Oceanic Technology, 2008, 25, 1623-1637.	1.3	18
76	Reply to "Comment on 'Seismomagnetic Effects from the Long-Awaited 28 September 2004 M 6.0 Parkfield Earthquake' by M. J. S. Johnston, Y. Sasai, G. D. Egbert, and R. J. Mueller" by P. Varotsos and S. Uyeda. Bulletin of the Seismological Society of America, 2008, 98, 2090-2093.	2.3	0
77	Scale Evolution of Finite-Amplitude Instabilities on a Coastal Upwelling Front. Journal of Physical Oceanography, 2007, 37, 837-854.	1.7	9
78	The impact of the M2 internal tide on data-assimilative model estimates of the surface tide. Ocean Modelling, 2007, 18, 210-216.	2.4	7
79	Representerâ€based variational data assimilation in a nonlinear model of nearshore circulation. Journal of Geophysical Research, 2007, 112, .	3.3	23
80	Data space conjugate gradient inversion for 2-D magnetotelluric data. Geophysical Journal International, 2007, 170, 986-994.	2.4	25
81	Empirical orthogonal function analysis of magnetic observatory data: Further evidence for nonâ€axisymmetric magnetospheric sources for satellite induction studies. Geophysical Research Letters, 2006, 33, .	4.0	26
82	Seismomagnetic Effects from the Long-Awaited 28 September 2004 M 6.0 Parkfield Earthquake. Bulletin of the Seismological Society of America, 2006, 96, S206-S220.	2.3	45
83	Verification studies for a z-coordinate primitive-equation model: Tidal conversion at a mid-ocean ridge. Ocean Modelling, 2006, 14, 257-278.	2.4	21
84	Estimating Open-Ocean Barotropic Tidal Dissipation: The Hawaiian Ridge. Journal of Physical Oceanography, 2006, 36, 1019-1035.	1.7	86
85	Constraints on mantle anelasticity from geodetic observations, and implications for theJ2anomaly. Geophysical Journal International, 2006, 165, 3-16.	2.4	74
86	Mapping nonlinear shallow-water tides: a look at the past and future. Ocean Dynamics, 2006, 56, 416-429.	2.2	35
87	Modeling Bottom Mixed Layer Variability on the Mid-Oregon Shelf during Summer Upwelling. Journal of Physical Oceanography, 2005, 35, 1629-1649.	1.7	17
88	Interpretation of two-dimensional magnetotelluric profile data with three-dimensional inversion: synthetic examples. Geophysical Journal International, 2005, 160, 804-814.	2.4	129
89	A Brief Overview of Tides in the Indonesian Seas. Oceanography, 2005, 18, 74-79.	1.0	75
90	Assimilation of Ship-Mounted ADCP Data for Barotropic Tides: Application to the Ross Sea. Journal of Atmospheric and Oceanic Technology, 2005, 22, 721-734.	1.3	29

#	Article	IF	CITATIONS
91	Three-dimensional magnetotelluric inversion: data-space method. Physics of the Earth and Planetary Interiors, 2005, 150, 3-14.	1.9	380
92	Distant effect of assimilation of moored currents into a model of coastal wind-driven circulation off Oregon. Journal of Geophysical Research, 2005, 110, .	3.3	20
93	Assimilation of moored velocity data in a model of coastal wind-driven circulation off Oregon: Multivariate capabilities. Journal of Geophysical Research, 2005, 110, .	3.3	34
94	Three-dimensional inversion for Network-Magnetotelluric data. Earth, Planets and Space, 2004, 56, 893-902.	2.5	42
95	Numerical modeling of the global semidiurnal tide in the present day and in the last glacial maximum. Journal of Geophysical Research, 2004, 109, .	3.3	240
96	Local time effects in satellite estimates of electromagnetic induction transfer functions. Geophysical Research Letters, 2004, 31, .	4.0	15
97	Geophysical images of the creeping segment of the San Andreas fault: implications for the role of crustal fluids in the earthquake process. Tectonophysics, 2004, 385, 137-158.	2.2	83
98	The Global S ₁ Tide. Journal of Physical Oceanography, 2004, 34, 1922-1935.	1.7	70
99	Tidal Models in a New Era of Satellite Gravimetry. Space Science Reviews, 2003, 108, 271-282.	8.1	55
100	Tidal currents on the central Oregon shelf: Models, data, and assimilation. Journal of Geophysical Research, 2003, 108, .	3.3	43
101	Semi-diurnal and diurnal tidal dissipation from TOPEX/Poseidon altimetry. Geophysical Research Letters, 2003, 30, n/a-n/a.	4.0	203
102	Tidal Models in a New Era of Satellite Gravimetry. Space Sciences Series of ISSI, 2003, , 271-282.	0.0	5
103	From Tides to Mixing Along the Hawaiian Ridge. Science, 2003, 301, 355-357.	12.6	312
104	The M2 Internal Tide off Oregon: Inferences from Data Assimilation. Journal of Physical Oceanography, 2003, 33, 1733-1757.	1.7	81
105	Deviation of Long-Period Tides from Equilibrium: Kinematics and Geostrophy. Journal of Physical Oceanography, 2003, 33, 822-839.	1.7	50
106	Efficient Inverse Modeling of Barotropic Ocean Tides. Journal of Atmospheric and Oceanic Technology, 2002, 19, 183-204.	1.3	2,947
107	Data Assimilation in a Baroclinic Coastal Ocean Model: Ensemble Statistics and Comparison of Methods. Monthly Weather Review, 2002, 130, 1009-1025.	1.4	23
108	A Modeling Study of the Three-Dimensional Continental Shelf Circulation off Oregon. Part II: Dynamical Analysis. Journal of Physical Oceanography, 2002, 32, 1383-1403.	1.7	49

#	Article	IF	CITATIONS
109	Numerical accuracy of magnetotelluric modeling: A comparison of finite difference approximations. Earth, Planets and Space, 2002, 54, 721-725.	2.5	62
110	A Modeling Study of the Three-Dimensional Continental Shelf Circulation off Oregon. Part I: Model–Data Comparisons. Journal of Physical Oceanography, 2002, 32, 1360-1382.	1.7	79
111	Assimilation of surface velocity data into a primitive equation coastal ocean model. Journal of Geophysical Research, 2002, 107, 5-1.	3.3	181
112	Magnetotelluric imaging of the creeping segment of the San Andreas Fault near Hollister. Geophysical Research Letters, 2002, 29, 1-1.	4.0	53
113	On the Generation of ULF Magnetic Variations by Conductivity Fluctuations in a Fault Zone. Pure and Applied Geophysics, 2002, 159, 1205-1227.	1.9	25
114	Processing And Interpretation Of Electromagnetic Induction Array Data. Surveys in Geophysics, 2002, 23, 207-249.	4.6	59
115	Error spectrum for the global M2ocean tide. Geophysical Research Letters, 2001, 28, 21-24.	4.0	29
116	Estimates of M2tidal energy dissipation from TOPEX/Poseidon altimeter data. Journal of Geophysical Research, 2001, 106, 22475-22502.	3.3	359
117	On the stability of magnetotelluric transfer function estimates and the reliability of their variances. Geophysical Journal International, 2001, 144, 65-82.	2.4	58
118	Assimilation of Surface Current Measurements in a Coastal Ocean Model. Journal of Physical Oceanography, 2000, 30, 2359-2378.	1.7	18
119	Significant dissipation of tidal energy in the deep ocean inferred from satellite altimeter data. Nature, 2000, 405, 775-778.	27.8	688
120	Correction to "DC trains and Pc3s: Source effects in mid-latitude geomagnetic transfer functions―by Gary D. Egbert, Markus Eisel, O. Sierra Boyd, and H. Frank Morrison. Geophysical Research Letters, 2000, 27, 1565-1565.	4.0	0
121	An efficient dataâ€subspace inversion method for 2-D magnetotelluric data. Geophysics, 2000, 65, 791-803.	2.6	360
122	DC trains and Pc3s: Source effects in mid-latitude geomagnetic transfer functions. Geophysical Research Letters, 2000, 27, 25-28.	4.0	29
123	Along strike variations in the electrical structure of the San Andreas Fault at Parkfield, California. Geophysical Research Letters, 2000, 27, 3021-3024.	4.0	112
124	Ocean mixing studied near Hawaiian Ridge. Eos, 2000, 81, 545.	0.1	27
125	High-resolution electromagnetic imaging of the San Andreas Fault in central California. Journal of Geophysical Research, 1999, 104, 1131-1150.	3.3	109
126	Internal structure of the San Andreas fault at Parkfield, California. Geology, 1997, 25, 359.	4.4	161

#	Article	IF	CITATIONS
127	Accuracy assessment of recent ocean tide models. Journal of Geophysical Research, 1997, 102, 25173-25194.	3.3	255
128	The flux of tidal energy across latitude 60°S. Geophysical Research Letters, 1997, 24, 543-546.	4.0	7
129	Robust multiple-station magnetotelluric data processing. Geophysical Journal International, 1997, 130, 475-496.	2.4	446
130	Tidal data inversion: interpolation and inference. Progress in Oceanography, 1997, 40, 53-80.	3.2	112
131	A TOPEX/POSEIDON global tidal model (TPXO.2) and barotropic tidal currents determined from long-range acoustic transmissions. Progress in Oceanography, 1997, 40, 337-367.	3.2	61
132	Diurnal/semidiurnal polar motion excited by oceanic tidal angular momentum. Journal of Geophysical Research, 1996, 101, 20151-20163.	3.3	80
133	Data assimilation methods for ocean tides. Elsevier Oceanography Series, 1996, , 147-179.	0.1	35
134	Single station magnetotelluric impedance estimation: Coherence weighting and the regression Mâ€estimate. Geophysics, 1996, 61, 964-970.	2.6	65
135	Diurnal/semidiurnal oceanic tidal angular momentum: Topex/Poseidon Models in comparison with Earth's rotation rate. Geophysical Research Letters, 1995, 22, 1993-1996.	4.0	19
136	TOPEX/POSEIDON tides estimated using a global inverse model. Journal of Geophysical Research, 1994, 99, 24821.	3.3	1,090
137	Imaging crustal structure in southwestern Washington with small magnetometer arrays. Journal of Geophysical Research, 1993, 98, 15967-15985.	3.3	25
138	Noncausality of the discreteâ€ŧime magnetotelluric impulse response. Geophysics, 1992, 57, 1354-1358.	2.6	21
139	Sampling bias in VGP longitudes. Geophysical Research Letters, 1992, 19, 2353-2356.	4.0	24
140	Very long period magnetotellurics at Tucson Observatory: Implications for mantle conductivity. Journal of Geophysical Research, 1992, 97, 15099-15112.	3.3	75
141	Very long period magnetotellurics at Tucson Observatory: Estimation of impedances. Journal of Geophysical Research, 1992, 97, 15113-15128.	3.3	36
142	On the synthesis of a large geomagnetic array from small overlapping arrays. Geophysical Journal International, 1991, 106, 37-51.	2.4	5
143	Comments On â€ [~] Concerning dispersion relations for the magnetotelluric impedance tensor' By E. Yee and K. V. Paulson. Geophysical Journal International, 1990, 102, 1-8.	2.4	35
144	A comparison of techniques for magnetotelluric response function estimation. Journal of Geophysical Research, 1989, 94, 14201-14213.	3.3	201

#	Article	IF	CITATIONS
145	Multivariate analysis of geomagnetic array data: 1. The response space. Journal of Geophysical Research, 1989, 94, 14227-14247.	3.3	49
146	Multivariate analysis of geomagnetic array data: 2. Random source models. Journal of Geophysical Research, 1989, 94, 14249-14265.	3.3	16
147	Stochastic Modeling of the Spaceâ€Time Structure of Atmospheric Chemical Deposition. Water Resources Research, 1986, 22, 165-179.	4.2	34
148	Multiple state stochastic models for the long-range transport and removal of atmospheric tracers. Quarterly Journal of the Royal Meteorological Society, 1986, 112, 843-865.	2.7	0
149	Robust estimation of geomagnetic transfer functions. Geophysical Journal International, 1986, 87, 173-194.	2.4	512
150	Tides in the Weddell Sea. Antarctic Research Series, 0, , 341-369.	0.2	69